Modeling and Experimentation of Monocrystalline Photovoltaic Module Performance with Flat Mirror Reflectors in Elbida Climate Conditions

Tarek.A.Hamad[1], Ahmed.A.Rased*[2], Yousif.H.Habib[1], Fouzi.M. Mossa[2]

[1] Department of Sustainable and Renewable Energy Engineering Omar Al-Mukhtar University, Libya
[2] Department of Mechanical Engineering Omar Al-Mukhtar University, Libya

(E-mail: ahmed.adil@omu.edu.ly,Tarek.Hamad@omu.edu.ly,Yousif.Hamad@omu.edu.ly ,fouzi.mohamed@oum.edu.ly)

ABSTRACT – The purpose of this paper is to give an outline of a method for optimizing solar panel performance in the presence of solar tracking mirrors in order to maximize energy output. Under the climate circumstances of Elbieda, as well as to examine the primary influence of cell temperature on the performance of mono-crystalline modules with a mirror reflector. For the photovoltaic system with flat mirror reflectors, a mathematical model has been developed to predict solar radiation. The components of solar radiation [global, direct, and diffuse], geometric factors, and geographical features of a PV installation are included in the model. In addition, to calculate the temperature of the cells. Where meteorological parameters such as ambient temperature, slope radiation, and wind speed are used to apply the energy balancing technique. On a specific day in July, the tests were carried out. The findings of the modeling simulation were compared to measurements taken during two periods, with and without the use of a reflector. For a traditional PV system and a PV reflector system, the coefficient of determination (R2) was 98.7% and 97% , respectively. In both situations, the mean bias error (MBE) values were less than 1%. The root means square error (RMSE) was 26.774% , 36.914% respectively in both cases. The estimated results were validated by comparing the results obtained for the measured slope surface irradiance and the measured unit cell temperature. The addition of flat mirror reflectors to successfully listed PV panels was extremely effective in detecting solar irradiance, resulting in positive findings of fitted parameters.

Keywords: Photovoltaic, Mirror, Cell temperature, Elbida, Performance, Modeling.

1. INTRODUCTION

Solar cells convert sunlight into electrical energy, making them a renewable energy source. Solar panels are made up of a group of solar cells with a greater voltage and current than a single cell. Solar panels are suitable for usage in locations with abundant sunlight. Solar panels also provide a number of advantages, including no pollution during the conversion of solar energy to electrical power and low maintenance costs. It's also advantageous since sunlight has the highest power density of all renewable energy sources. However, the cost of the solar panel device and installation is rather high, making the initial investment quite pricey. As a result, users want Solar panel performance optimization in order to generate as much electricity as feasible. The maximum amount of electrical power that a solar

Panel can produce shows that the solar panels are performing at their best. The power production of solar panels will rise as solar radiation increases. Reflectors can increase the amount of solar energy that reaches a solar panel. It produces reflected light that is directed toward the solar panel. As a consequence, the solar panels may receive light from two directions. In addition, the reflector should be the same size as the solar panels, if not slightly larger, to ensure that all reflected light lands on the solar panel's surface [1]. Previous study has demonstrated that a planar reflector system can increase the intensity of solar radiation [2]. Reflecting light onto the solar panel, these reflectors will improve electrical power output. Concentrating mirror boosters are a new technology that is gaining popularity. Because of its low price and wide availability, this option is the most appealing. Despite this, low-cost and Cost-effective solutions are required to make their installation more realistic [3]. In 1958, Tabor [4] was the first to use a reflector to increase the solar energy collection area by reflecting additional solar radiation onto it. Employing a reflector to produce electricity from a PV system is more cost-effective than using additional PV panels to generate the same amount of power. Adding planar reflectors, according to [5] is a low-cost alternative that can boost produced energy by up to 35 % on clear days. Flat booster reflectors were tested in a variety of PV systems as well as a variety of alternate layouts in [6]. For example, at SIRTA [7], the ALEPH project (Amelioration of photovoltaic efficiency) was implemented with the objective of boosting system production by installing inter-row planar reflectors. In addition, TENKSOLAR has developed a planar reflector industrial PV system. Bloomington, Indiana [8] .demonstrates the use of flat wide-area reflectors. Flat reflectors have also been shown to improve incident sun flux in solar thermal systems in other research. Installing flat reflectors can increase annual irradiance by 8% to 17 % in Sweden [9], according to a study based on evenly dispersed radiation]. Irradiance can be increased by up to 9% with an optimum fixed PV-reflector arrangement, according to research done in various sites around the United States [10]. When compared to parabolic concentrators, one advantage of a planar reflector PV system is that it has a lower concentration. As a result, the temperature negative effect is not as strong with flat reflectors, and so no cooling operation is required, lowering the system's cost [11]. Furthermore, unlike CPV technology, which requires great precision and dependability for tracking systems, PV reflector systems do not require accurate sun tracking equipment, resulting in higher costs. This project's mission is to develop a POA irradiance estimation model for a PV system using mirror reflectors. The system's efficiency is investigated in the context of geometrical optimization case studies under Elbieda Climate Conditions. To do this, a MATLAB code is written to recognize the following**:**

- To compare the energy output of solar panels with and without a mirror reflector under a variety of boundary conditions, including latitude, PV module orientation, and panel and mirror tilt angles.
- Examine the impact of cell temperature on PV module performance while using a mirror reflector and when not using one.

2. Methodology

2.1 Experimental investigation

The study will be carried out in the Department of Mechanical Engineering at the University of Omar Al-Mokhtar's Faculty of Engineering in

Elbida, Libya (32.7[redacted]6 N; 21.[redacted]75 ° E). Because the current study is focusing on the influence of the reflector on fixed PV systems, the solar module and reflector are installed at optimal tilt

angle [redacted]51 for the site. Two monocrystalline photovoltaic modules (Type E850) with a peak power rating of 85W will be employed in this study's experimental setup to acquire the experimental findings. The first module is under normal operating circumstances and will be used as a reference, while the other (PV) is a PV module test conditions of $1000 W/m^2$ irradiation, $25C$ cell temperature, and 1.5 air mass, this module has 36 cells with short circuit current and open circuit voltage of $5.20A$ and $22V$, respectively (AM). Table 1 contains further information about the PV module's specs. For each solar panel in this study, one reflector is employed. The reflector is 1.23 m long and 0.55 m wide. It's set up in such a way that there are no shadows cast on the solar panel. A flat reflector constructed of glass is used in this experiment. The monocrystalline (m-Si) PV module with and without a mirror reflector has been designed to have the experimental results of this study as shown in (Figure 1).

Table 1: Specifications of the PV module. Electrical Specification

Model	TE 850
Peak power (P_m)	85 W
Short circuit current (I_{sc})	5.20 A
Open circuit voltage (V_{oc})	22.0V
Max. power current (I_m)	4.80A
Max. Power voltage (V_m)	17.7 V
Panel Efficiency	13%
Module area	0.684 m^2

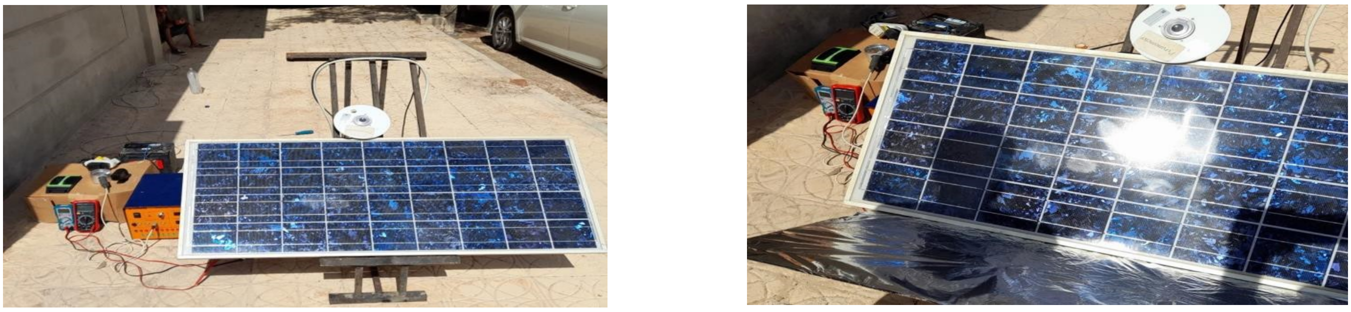

Figure 1: Photograph of the experimental setup.

Measurements were taken on a clear day in July 2021 from 8 : 00 am to 5 : 00 pm. for the aim of evaluating PV module performance, and experimental data was collected every half hour. During the testing period, the measured parameters such as slope irradiance, ambient temperature, cell temperature, voltage, current, and wind speed were critical and needed to be carefully examined. A pyranometer (RK200-03) was used to measure the intensity of solar radiation at the same tilt angle as the PV module. Module's current and voltage measurements in order to offer precise information on the PV module's power output. The wind speed was measured using an anemometer. A thermocouple was placed on the front surface of the PV module using thermal tape to detect cell temperature. The ambient temperature was measured using another thermocouple. The data logger and signals converter device were used to collect all of the data. (Figure 2) depicts the configuration of the experimental set-up with several instruments.

2.2. Mathematical Modelling

The total solar radiation on the PV surface with the tilted plane, angle b is the sum of direct solar radiation travelling in a straight line from the sun to the earth's surface, diffuse solar radiation scattered in the atmosphere and reaching the earth's surface, and reflected radiation from the ground (Figure. 3a). The direct and diffuse irradiances hitting the mirror's surface, which are then reflected on the PV module, will be added in the case of a system with a flat reflector (Figure. 3b). For the purposes of this study, a MATLAB software was used to develop a PV module model, which takes solar radiation and the ambient temperature of the location as data to estimate:

- The overall irradiance of a reflector-equipped panel.
- The panel's temperature, which is impacted by increasing irradiation.
- The electrical output that is predicted.

For the study, a one-hour time step was employed. According to methods given in [13], the hourly solar radiation data were generated from monthly insolation data.

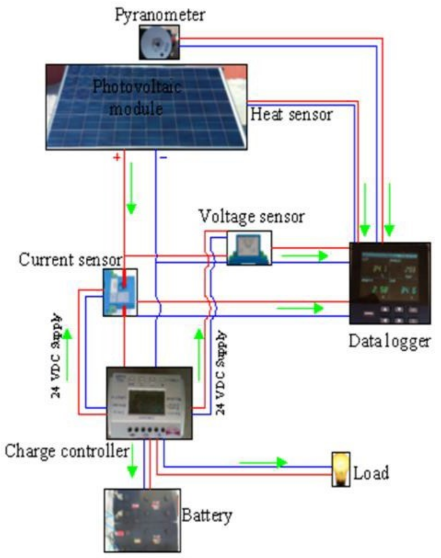

Figure 2: Layout of the experimental setup.

2.2.1 Photovoltaic Irradiation model for the PV system without a mirror reflector

The total of solar radiation from the sky (beam and diffuse), the ground (reflected), and the reflector equals the irradiance on the PV panel (specular and diffuse). The irradiance on a slanted surface is investigated in terms of direct (beam, H_{dir-pv}), diffuse from the sky ($H_{diff-pv}$), and reflected from the ground ($H_{ref-gr-pv}$), which are

$$H_{total-pv} = (H_{total-hor} - H_{diff-hor})*\frac{\cos(\theta)}{\cos(\theta_z)} + H_{diff-hor}*\frac{1+\cos(\beta)}{2} + H_{total-hor}*\rho_G*\frac{1-\cos(\beta)}{2} \quad (1)$$

The positioning of a reflector in front of a PV panel has the potential to impact both diffuse and ground reflected incident solar energy. Because of the modest slope of the reflector, the first impact is ignored, while the second is approximated by suitably adjusting the relevant term:

$$H_{ref-gr-pv} \approx H_{total-hor} * \rho_G \left[\frac{1-\cos(\beta)}{2} - F_{pv\_R}\right] \quad (2)$$

From the reflector to the PV module, the view factor is as follows:

$$F_{R\_PV} = \frac{n + p - \sqrt{n^2 + p^2 - 2*p*\cos(\psi)}}{2*p} \quad (3)$$

with $F_{PV\_R} = F_{R\_PV} * (p/n)$. The fundamental formulae for reflected radiation were provided in [14], although they only applied to solar noon (identical solar and module azimuth angles). However, in any other scenario, the computations become more difficult. The angle of incidence of the reflected beam to the panel is computed as follows in the typical situation. The solar altitude and azimuth angles are computed first, as seen from the reflector's surface (in Figure 4, the surface ACE is horizontal, and the surface ABD is the reflector's surface). It is self-evident that $\zeta = BAC$ $\gamma_s = CAE$, $\alpha_s = FAE$.

$$\alpha_1 = \alpha_s - a\tan\left[\tan(\zeta)*\cos(\gamma_s)\right] \quad (4)$$

$$\gamma_1 = a\tan\left[\cos(\zeta)*\tan(\gamma_s)\right] \quad (5)$$

The following formula is used to determine the quantities m_1, m_2 and m_3:

$$m_1 = \sqrt{\tan^2(\gamma_1) + \frac{1}{\tan^2(\psi + \alpha_{p1})}} \quad (6)$$

$$m_2 = \frac{\cos(\alpha_{p1})}{\sin(\psi + \alpha_{p1})} \quad (7)$$

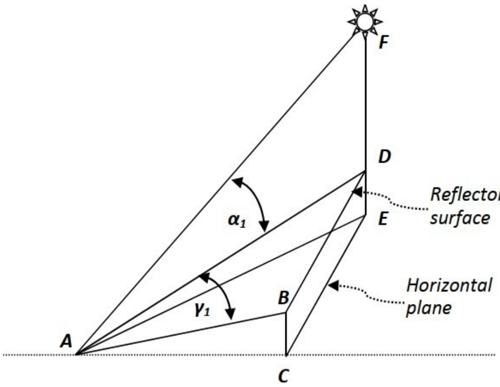

Figure 3: The geometry of the sunlight, mirror and PV panel. In surface ACE is horizontal, and surface ABD is that of the reflector. [13].

$$m_3 = \sqrt{\tan^2(\gamma_1) + \frac{\sin^2(\psi)}{\sin^2(\psi + \alpha_{p1})}} \quad (8)$$

Where $\alpha_{p1} = (\alpha_p - \zeta)$, α_p is the solar profile angle (the projection of the solar altitude angle on a surface vertical to the PV panel and the horizontal plane), which is provided by the relationship:

$$\alpha_p = a\tan\left(\frac{\tan(\alpha_s)}{\cos(\gamma_s)}\right) \quad (9)$$

Finally, the angle of incidence of the reflected beam on the PV panel is computed as follows:

$$\theta' = a\cos\left(\frac{m_2^2 + m_3^2 - m_1^2}{2 * m_2 * m_3}\right) \quad (10)$$

The corresponding irradiance is:

$$H_{dir-REF-pv} = \rho * G_{dir-hor} * \frac{\cos(\theta'')}{\cos(\theta)} \quad (11)$$

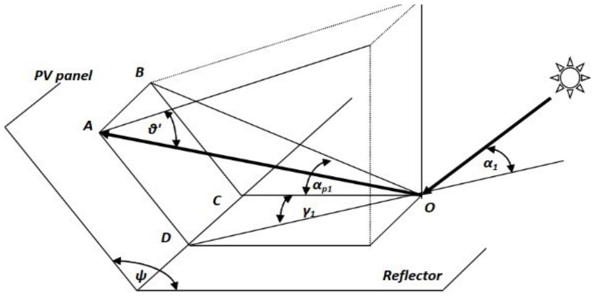

Figure. 4: The geometry of the sunlight, mirror and PV panel. [13].

With ρ the reflector's reflectivity, $G_{dir-hor}$ the horizontal plane's beam radiation, and the sun's zenith angle as inputs. This ρ is the specular reflected radiation from the reflector to the PV panel (with crystalline silicon panels, this extra radiation is only taken into account when the entire PV panel is uniformly lit by the reflector; see Figure 5 for further information). Finally, diffuse reflected solar energy is taken into account (albeit it is of small relevance). This is due to diffuse and reflected radiation from the sky and the ground, which falls on the reflector and is reflected as diffuse radiation. The relation approximates the portion of diffuse reflected radiation that reaches the PV panel:

$$H_{ref\_diff\_pv} \cong (1 - F_{R\_PV}) * \left[H_{diff\_hor} * \frac{1+\cos(\zeta)}{2} + H_{tot\_hor} * \rho_G * \frac{1-\cos(\zeta)}{2} \right] * \rho * F_{pv\_R} \quad (12)$$

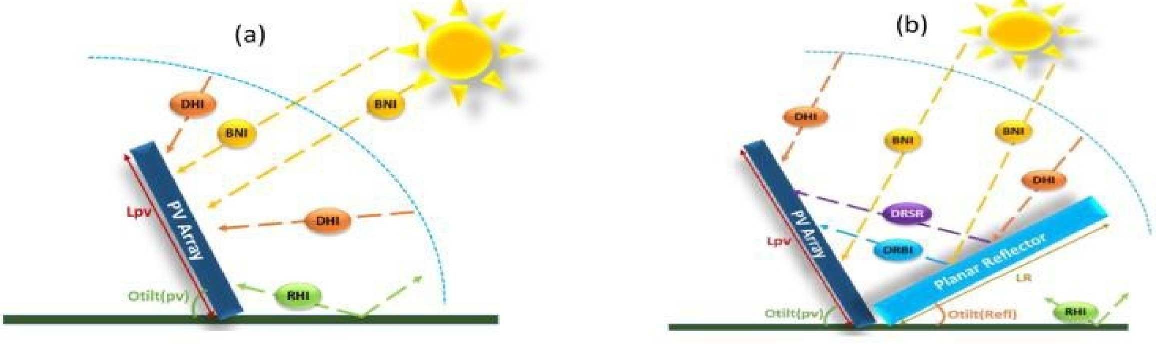

Figure: 5: Irradiances characterizing a classical PV system architecture (a) and a PV-reflector system architecture (b) [12].

2.2.2 Effect of temperature

According to the relationship [14], an increase in irradiance induces an increase in cell temperature.

$$T_{CELL} = T_{AIR} + \frac{(NOCT - 25)}{800} * G \qquad (13)$$

Where T_{AIR} is the ambient temperature ([redacted]), NOCT is (the normal operating cell temperature) ([redacted]) and G is the panel's irradiance (W/m^2). Increased cell temperature produces simultaneous increases in current and decreases in voltage, with the net impact of both changes being a small loss in panel efficiency according to the relationship.

2.2.3 Electrical model

- A photovoltaic module's power relationship is as follows:

$$P = I \times V \qquad (14)$$

- The following formula is used to calculate electrical efficiency:

$$\eta = \eta_{ref} * \left(1 - \beta_{ref}\left(T_C - T_{ref}\right)\right) \qquad (14)$$

Where η_{ref} is the reference efficiency under normal conditions and β_{ref} is the temperature coefficient of cell efficiency which varies depending on the materials used in the PV module; the value for silicon cells is 0.00045/K [15].

3. Results and discussion

3.1. Experimental results

The hourly variation of ambient temperature, cell temperature, solar irradiance, and power output obtained from the experimental work during the test day for the PV module are shown in Figures 2.and 3. As it can be seen from the figures, the cell temperature, slope irradiance, and electrical power output from the PV module reach the highest at 11:00, with values 42.52039594oC, 969 W/m2, and 48.74 W, respectively, whilst ambient temperature is about 34.055 oC. Figures 3 and 4 show the hourly variation of ambient temperature, cell temperature, slope irradiance, outlet air temperature, and power output based on the experimental work during the test day for the PV with a mirror system. It can be observed from the figures that the cell temperature, solar irradiance and electrical power output from the PV module reaches the maximum at 11:00, with values of 49.59oC, 1167.69467W/m2, and 59.21 W, respectively. To the highest ambient temperature value of 34.055 ^{o}C.

3.2. Validation

The computed values of slope irradiance (PV with mirror), cell temperature (PV with mirror), and solar cell temperature from the created model have been verified against experimental data. In addition, the slope irradiance was confirmed using measured data collected under various climatic conditions. To do so, a comparison of the calculated and experimental data is made in terms of their correctness, which is done using well-known statistical markers. [16]. in this part, we'll go through the parameters that were utilized to evaluate the forecasts. For evaluating the accuracy of solar irradiance, cell

Temperature, and PV power predictions, we utilize mean absolute error (MAE), root mean square error (RMSE), mean absolute percentage error (MAPE), correlation coefficient, and skill the score.

$$MAE = \frac{\sum_{i=1}^{N} \left| y_i - y_i \right|}{N} \qquad (15)$$

$$MAPE = \frac{\sum_{i=1}^{N} \left| y_i - y_i \right|}{N} \times 100\% \qquad (16)$$

The MAE and $MAPE$ have smaller values, indicating that the forecast is more accurate.

$$RMSE = \sqrt{\frac{\sum_{i=1}^{N}\left(y_i - y_i\right)^2}{N}} \qquad (17)$$

Smaller $RMSE$ values imply that the forecast is more accurate than the measured value.

$$R = \frac{\sum_{i=1}^{N}\left(y_i - \overline{y}\right)\left(y_i - \overline{y}\right)}{\sqrt{\sum_{i=1}^{N}\left(y_i - \overline{y}\right)^2 \sum^{N}\left(y_i - \overline{y}\right)^2}} \qquad (18)$$

In the range $-1 \le R \le 1$, the correlation coefficient is defined as:

- If $R = -1$ is true, y_i and y_i have a perfect negative linear connection.
- If $R = 1$ is true, y_i and y_i have a perfect positive linear connection.
- If $R = 0$ is true, y_i and y_i do not have a linear connection.

The experimental versus calculated values of slope irradiance, cell temperature during the test day for the PV module is shown in Figure 7. According to this figure, it is found that there is a good concordance between the experimental and the calculated results with a coefficient of determination (R2) = 0.9996, and the Root mean square error (RMSE) = 0.582.

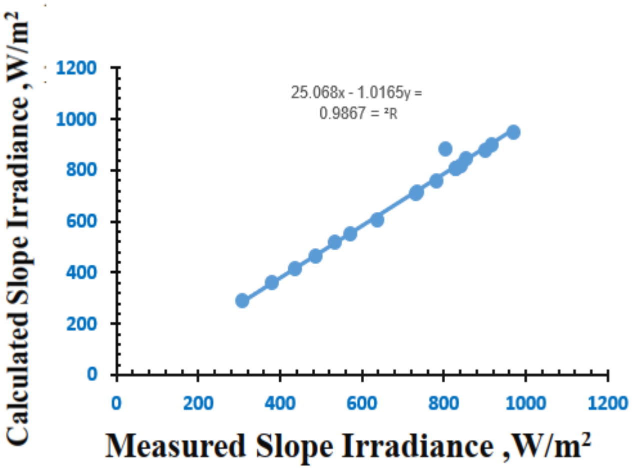

Figure 6: Experiment versus calculation of slope irradiance during the test period

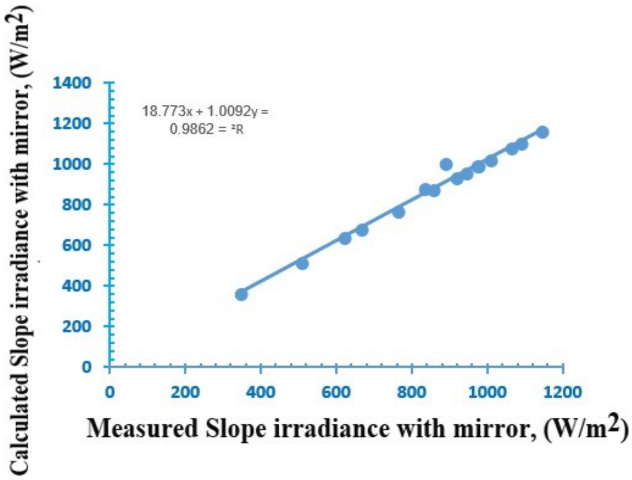

Figure 7: Experiment versus calculation of slope irradiance with mirror during the test period.

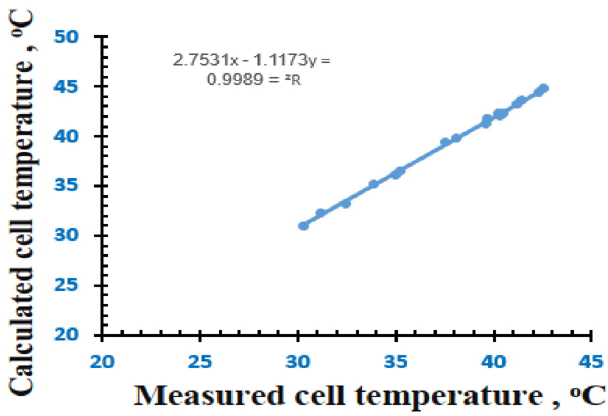

Figure 8: Experimental versus calculated values of cell temperature during the test day

3.3 Effect of temperature on PV module performance

It is well knowing that the efficiency of PV modules diminishes as module temperature rises. This leads to a reduction in overall solar power plant power output, particularly in hot climes, while other factors such as dust collection and PV deterioration also influence PV efficiency, necessitating corrective actions such as cooling and cleaning of PV modules.

However, the temperature effect on PV modules is not found to be especially important in this portion of the Himalayan area when ambient temperatures are low. In addition to the rise in temperature of PV modules caused by ambient temperature, reflected solar radiation falling on the PV module is expected to raise the temperature in comparison to a PV system without a mirror reflector, but the temperature rise in both cases is dependent on other factors such as location weather (ambient temperature, wind speed, humidity, etc.), reflector material, and so on. The PV efficiency will be affected by a rise in solar cell temperature. However, because the temperature rise caused by the reflector is modest, the effect on PV efficiency is unlikely to be significant in this study. The highest temperature rise in PV panels was determined to

be 49.59 [redacted]in this investigation, which is just 7 [redacted]ore than a PV system without a reflector. This is a significant finding because reflector-added PV modules may be utilized to generate additional electricity without compromising the modules' performance. Figure 13 depicts the expected electrical efficiency and cell temperature variations for each system throughout the measurement day.

CONCLUSIONS

The primary objective of this study is to compare the theoretical and empirical performance of monocrystalline modules with and without mirror reflectors. The model is validated through experiments. As a consequence of the current study, the following findings have been reached**:**

- A series of outdoor experiments were carried out on the two proposed schemas of the PV module with and without mirror, using the equipment provided by the energy laboratory at the University of engineering - Elbida.
- The observed solar irradiance on a sloping surface matches the model well, yielding promising coefficient of determination (R2), mean bias error (MBE), and root mean square error findings (RMSE).
- The results of the modelling simulation were compared to measurements made during two periods, one with and one without a reflector. The coefficients of determination (R2) for a standard PV system and a PV reflector system, respectively, were 98.7% and 97% . The mean bias error (MBE) values in both scenarios were less than 1%. In each of these situations, the root mean square error (RMSE) was 26.774% , 36.914%.
- The maximum temperature rise discovered in a PV panel with a reflector was 49.59 degrees Celsius. Because the effect of a mirror reflector on PV efficiency is modest, it is unlikely to have a major impact at this research location, which is in the mountainous Derna region with low ambient temperatures. However, this variation is site-specific, and it may be higher in hot regions where PV panel cooling is employed.
- A PV system with bottom reflectors, according to the research, enhances the power production capacity. In the case of large power plants, this would result in increased land usage efficiency and a reduction in the number of PV panels, decreasing installation and land costs while boosting revenue from the power Plant's energy output. More research is needed on this feature.

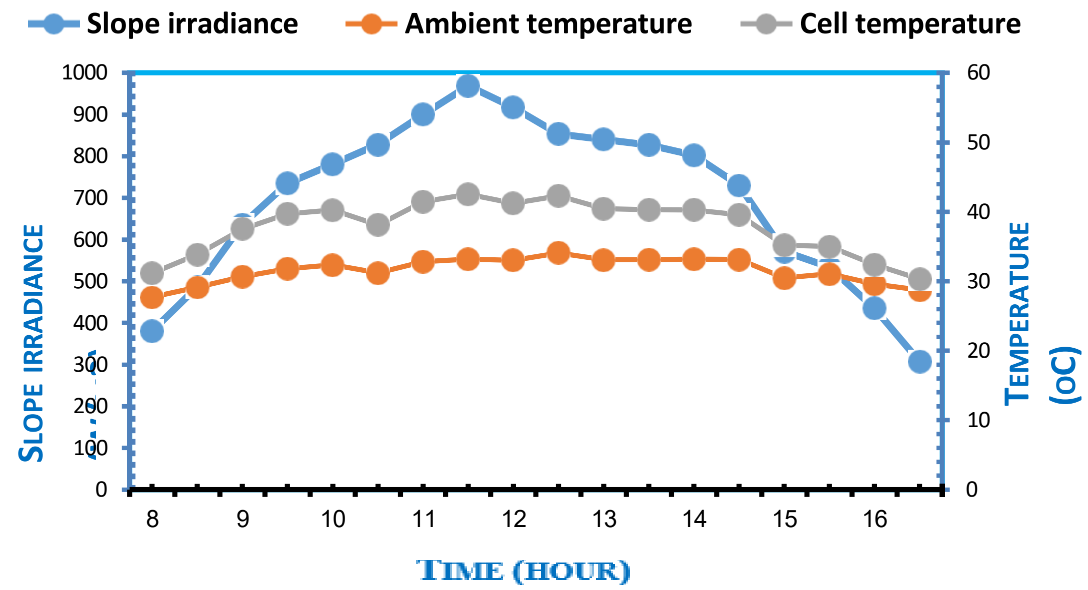

Figure 9: The ambient temperature, cell temperature, and slope irradiance Fluctuated during the PV module's test day.

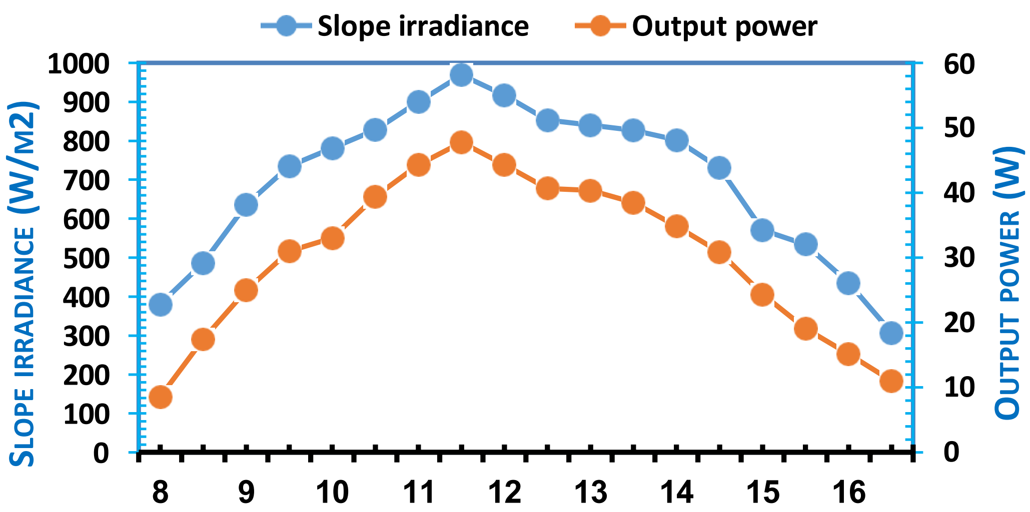

Figure 10: During the PV module's test day, the slope irradiance and power output varied.

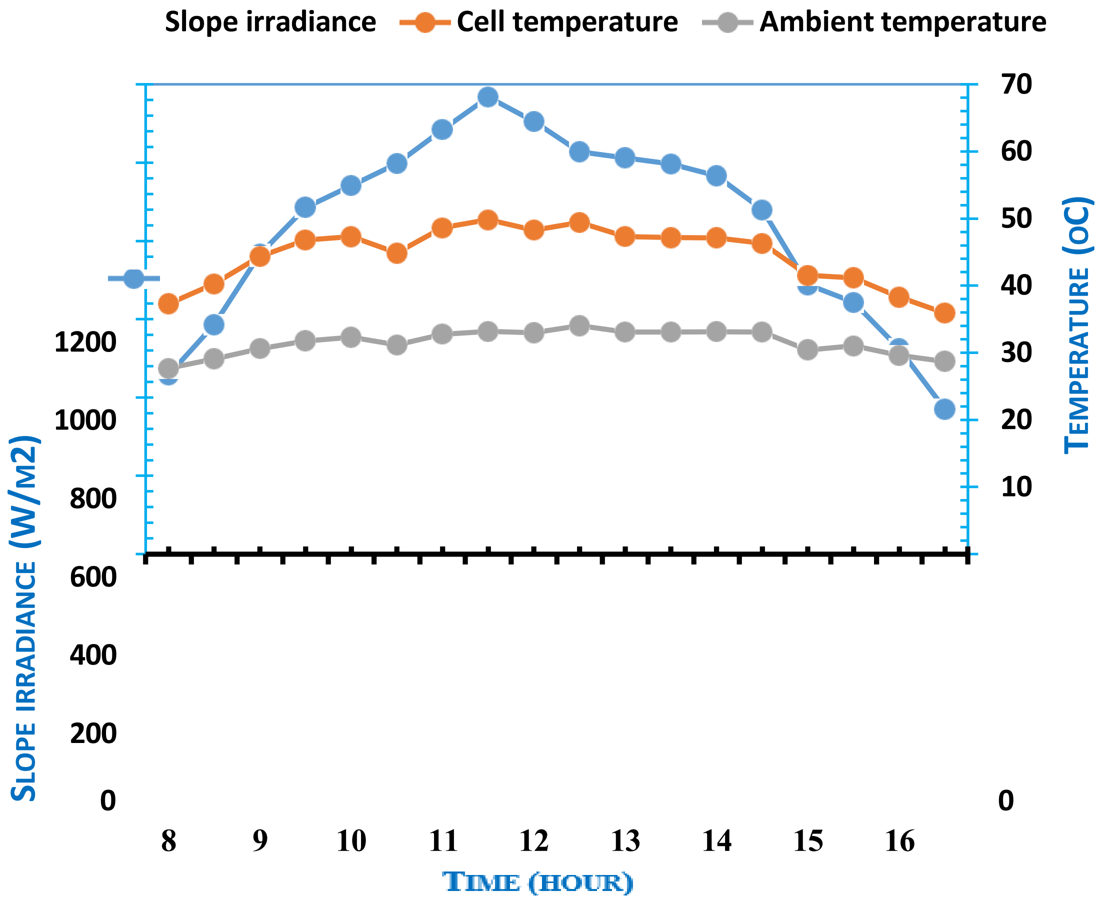

Figure 11: Variation of ambient temperature, cell temperature, and slope irradiance During the test day for the PV with mirror

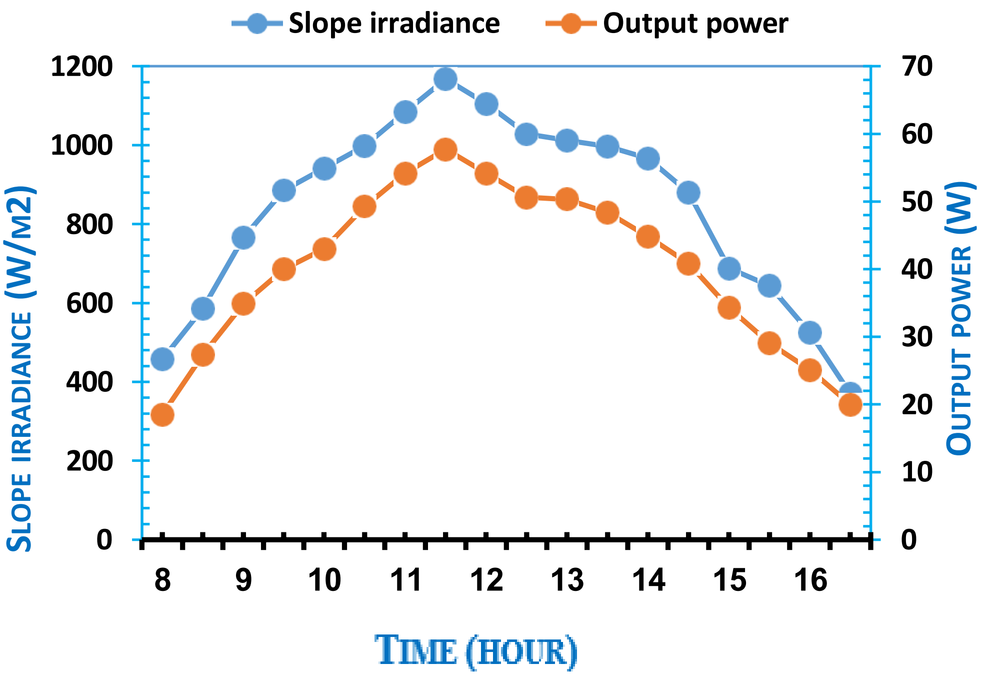

Figure 12: Variation of slope irradiance and power output during the test day for the PV with mirror.

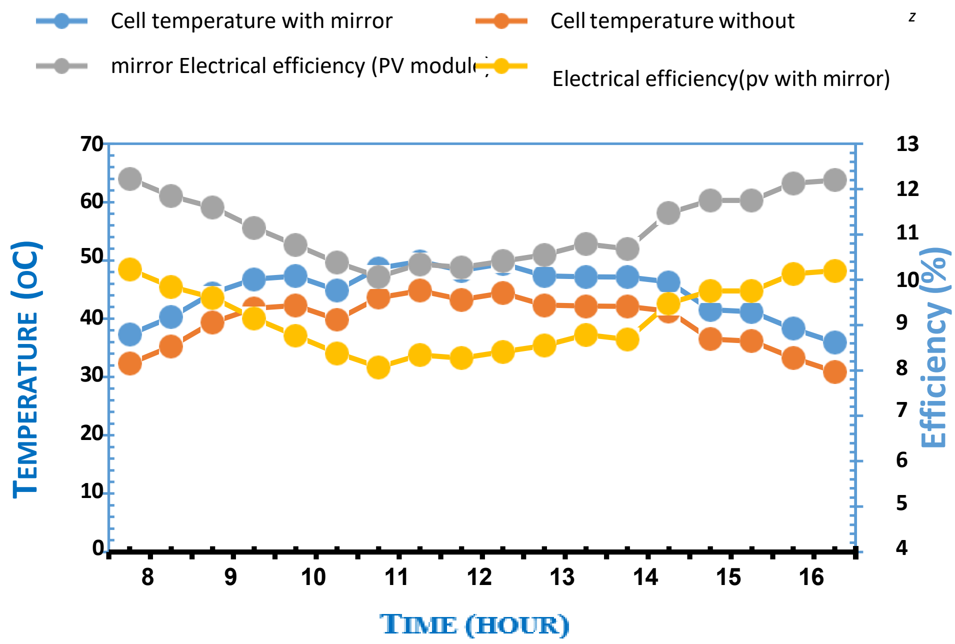

Figure 13: Variations of the predicted electrical efficiency and cell temperature for each System during the test day.

REFERENCES

[1] Setiawan, E. A., & Dewi, K. (2013). Impact of two types flat reflector materials on solar panel characteristics. *Science*, *2*, 188-199.

[2] Deline, C., Dobos, A., Janzou, S., Meydbray, J., & Donovan, M. (2013). A simplified model of uniform shading in large photovoltaic arrays. *Solar Energy*, *96*, 274-282.

[3] Khan, M. A., Ko, B., Alois Nyari, E., Park, S. E., & Kim, H. J. (2017). Performance evaluation of photovoltaic solar system with different cooling methods and a bi-reflector PV system (BRPVS): an experimental study and comparative analysis. *Energies*, *10*(6), 826.

[4] Tabor, H. (1958). Stationary mirror systems for solar collectors. *Solar Energy*, *2*(3-4), 27-33.

[5] Pavlov, M., Migan-Dubois, A., Bourdin, V., Pons, M., Haeffelin, M., & Badosa, J. (2015). Experimental and numerical study of the Influence of string mismatch on the yield of PV modules augmented by static planar reflectors. *IEEE Journal of Photovoltaics*, *5*(6), 1686-1691.

[6] Gelegenis, J. J., Axaopoulos, P., Misailidis, S., Giannakidis, G., Samarakou, M., & Bonaros, B. (2015). Feasibility for the use of flat booster reflectors in various photovoltaic installations. *International Journal of Renewable Energy Research (IJRER)*, *5*(1), 82-98.

[7] Badosa, J., Bourdin, V., Haeffelin, M., Mambrini, T., Migan-Dubois, A., & Nassar, J. (2015, September). Multi-technology photovoltaic module test bench on the SIRTA meteorological and climate observatory. In *31st European PV Solar Energy Conference and Exhibition*.

[8] Modanese, C., Laine, H. S., Pasanen, T. P., Savin, H., & Pearce, J. M. (2018). Economic

advantages of dry-etched black silicon in passivated emitter rear cell (PERC) photovoltaic manufacturing. Energies, 11(9), 2337

[10] Rönnelid, M., Karlsson, B., Krohn, P., & Wennerberg, J. (2000). Booster reflectors for PV modules in Sweden. Progress in photovoltaics:

[11] Boyd, M. (2013). Analytical model for solar irradiance near a planar vertical diffuse reflector– Formulation, validation, and simulations. Solar Energy, 91, 79-92.

[12] Andrews, R., Pollard, A., & Pearce, J. (2013, June). Photovoltaic System Performance Enhancement With Non-Tracking Planar Concentrators: Experimental Results and Bi- Directional Reflectance Function (BDRF) Based Modelling. In IEEE 39th Photovoltaic Specialists Conference (PVSC).

[13] Nour, C. A., Migan-Dubois, A., Badosa, J., Bourdin, V., Marchand, C., & Akiki, T. (2020). Geometrical optimization for a photovoltaic installation equipped with flat reflectors based on plane of array estimations. EPJ Photovoltaics, 11.

[14] Duffie, J. A., & Beckman, W. A. (2013). Solar Radiation. Solar Engineering of Thermal Processes, 4th. Ed., Hoboken, New Jersey: Wiley, 12-20.

[15] Ross Jr, R. G., & Smokler, M. I. (1986). Flat-plate solar array project. Volume 6: Engineering sciences and reliability. Jet Propulsion Lab. Report.

16] Joshi, A. S., Tiwari, A., Tiwari, G. N., Dincer, I., & Reddy, B. V. (2009). Performance evaluation of a hybrid photovoltaic thermal (PV/T) (glass-to-glass) system. International Journal of Thermal Sciences, 48(1), 154-164.

[17] Durrani, S. P., Balluff, S., Wurzer, L., & Krauter, S. (2018). Photovoltaic yield prediction using an irradiance forecast model based on multiple neural networks. Journal of Modern Power Systems and Clean Energy, 6(2), 255-267.